Water Resources Research

RESEARCH ARTICLE
10.1029/2023WR036217

A High-Resolution, Daily Hindcast (1990–2021) of Alaskan River Discharge and Temperature From Coupled and Optimized Physical Models

Dylan Blaskey[1], Michael N. Gooseff[1], Yifan Cheng[2], Andrew J. Newman[2], Joshua C. Koch[3], and Keith N. Musselman[1,4]

[1]Insitute of Arctic and Alpine Research, University of Colorado, Boulder, CO, USA, [2]National Center for Atmospheric Research, Boulder, CO, USA, [3]U.S. Geological Survey Alaska Science Center, Anchorage, AK, USA, [4]Department of Geography, University of Colorado, Boulder, CO, USA

Key Points:

- Our model system produced an accurate, high-resolution, daily hindcast of Alaskan river temperature and discharge from 1990 to 2021
- We increased model performance by employing a new optimization of the River Basin Model and forcing it with a climate-land surface model
- A sensitivity analysis highlights important drivers of river temperatures in each region and the need for optimization

Supporting Information:

Supporting Information may be found in the online version of this article.

Correspondence to:

D. Blaskey,
dylan.blaskey@colorado.edu

Citation:

Blaskey, D., Gooseff, M. N., Cheng, Y., Newman, A. J., Koch, J. C., & Musselman, K. N. (2024). A high-resolution, daily hindcast (1990–2021) of Alaskan river discharge and temperature from coupled and optimized physical models. *Water Resources Research*, *60*, e2023WR036217. https://doi.org/10.1029/2023WR036217

Received 6 SEP 2023
Accepted 26 MAR 2024

Abstract Water quality and freshwater ecosystems are affected by river discharge and temperature. Models are frequently used to estimate river temperature on large spatial and temporal scales due to limited observations of discharge and temperature. In this study, we use physically based river routing and temperature models to simulate daily discharge and river temperature for rivers in 138 basins in Alaska, including the entire Yukon River basin, from 1990–2021. The river temperature model was optimized for ice free months using a surrogate-based model optimization method, improving model performance at uncalibrated river gages. A common statistical model relating local air and water temperature was used as a benchmark. The physically based river temperature model exhibited superior performance compared to the benchmark statistical model after optimization, suggesting river temperature model optimization could become more routine. The river temperature model demonstrated high sensitivity to air temperature and model parameterization, and lower sensitivity to discharge. Validation of the models showed a Kling-Gupta Efficiency of 0.46 for daily river discharge and a root mean square error of 2.04°C for daily river temperature, improving on the non-optimized physical model and the benchmark statistical model, which had root mean square errors of 3.24 and 2.97°C, respectively. The simulation shows that rivers in northern Alaska have higher maximum summer temperatures and more variability than rivers in the Central and Southern regions. Furthermore, this framework can be readily adapted for use across models and regions.

Plain Language Summary Accurate data on the volume and temperature of river water are essential for understanding how changing river conditions affect water quality and freshwater ecosystems. However, direct measurements of river parameters are often lacking, leading researchers to rely on models for estimation. In this study, we utilized advanced models and techniques to compute daily water volume and temperature in 138 basins across Alaska, including the entirety of the Yukon River basin, spanning from 1990 to 2021. Our findings indicated that rivers in northern Alaska exhibited higher maximum summer water temperatures and more significant temperature fluctuations compared to those in the central and southern regions. Our analysis highlighted that adjusting air temperature and the model's internal variables were crucial in minimizing errors in river temperature prediction. We improved the accuracy of the river temperature model by applying a technique to refine the model output based on the limited available river measurements. Comparing our enhanced model to a simpler statistical approach, we observed superior performance once the necessary adjustments were implemented.

1. Introduction

Air temperatures in Alaska are increasing four times faster than the global average (Rantanen et al., 2022). The rise in air temperature has led to substantial thawing of permafrost and glaciers, increased winter snowmelt, altered subsurface flow patterns, and shifted river seasonality (Blaskey et al., 2023; Koch et al., 2022; Li et al., 2022; Musselman et al., 2021; Yang et al., 2020). Water temperature in Alaska's largest rivers has also increased, impacting water quality, the growth rate and distribution of freshwater species, and biogeochemical cycling (Kaushal et al., 2010; Tornabene et al., 2020; Wanders et al., 2019; von Biela et al., 2022). For example, record-breaking air temperatures and drought in 2019 caused widespread mortality among returning salmon in the Yukon River (von Biela et al., 2022). The combination of low discharge and high water temperatures can prevent migrating salmon from accessing pools of colder water needed for survival (Frechette et al., 2018). When salmon

cannot migrate, the spiritual, cultural, social, and economic well-being of local and Indigenous people is affected (Carothers et al., 2021). Despite these ongoing changes and the resulting socioeconomic impacts, observation and modeling data of Alaskan river temperatures are rare.

River temperatures are spatially and temporally heterogeneous (Steel et al., 2017) primarily due to atmospheric and terrestrial energy fluxes. These fluxes are controlled by topography, groundwater inputs, hyporheic exchange, river stratification, flow velocity, and vegetation (Burkholder et al., 2008; Dugdale et al., 2015, 2017; Nielsen et al., 1994). However, capturing this heterogeneity is difficult because observational river temperature data are limited with typically low spatial and temporal resolutions (Watts et al., 2015). Therefore, river temperature models are frequently used to understand large-scale river temperature patterns and its physical drivers due to their continuous spatial and temporal data (Ruesch et al., 2012; Tung et al., 2006).

Many river temperature simulations rely solely on land surface models, lacking dynamic coupling between the land and atmosphere (e.g., Sun et al., 2015). However, coupled land and atmospheric models could enhance accuracy by providing a comprehensive representation of Arctic system processes (Lawrence et al., 2019). Furthermore, an enhanced physical representation of landscapes and land-atmosphere interactions bolsters the credibility of models in regional applications and community use (Giorgi, 2019). Climate and Earth System models are increasingly operating at higher spatial resolutions to improve physical process representation, addressing factors such as convection and orographic impacts (Reder et al., 2020). Despite these advancements, the optimization of parameters within complex Land Models lags due to uncertainties, structural errors, and missing process representations (Lehner et al., 2019). Alaska is a difficult region to model and is prone to high errors in both land surface and river temperature modeling due to sea ice dynamics, heterogenous permafrost, snow, complex terrain, and limited data (Cheng et al., 2023; Monaghan et al., 2018; Wanders et al., 2019). The Regional Arctic System Model (RASM) has been developed specifically for cold regions, so it excels in capturing diverse topography, realistically simulating seasonal snow, orographic precipitation patterns, and heterogeneous permafrost (Lawrence et al., 2019).

In river temperature modeling, errors cascade through modeling chains from the land surface model, through discharge model, and then to the river temperature model (van Vliet et al., 2012). Without highly accurate and high-resolution input data, errors surpass the subtle fluctuations in water temperature critical to sensitive aquatic organisms, rendering the data less useful (Tisseuil et al., 2012; van Vliet et al., 2013; Wanders et al., 2019). For instance, salmon, have a maximum thermal limit of around 18°C, but this limit varies by 2–3°C within the species at the same life stage (Coutant, 1999; Mayer et al., 2023; Pörtner & Farrell, 2008). Few models can operate within this error tolerance from headwaters to the mouth of the river, which is needed to capture the thermal effects on migratory fish species (Lee et al., 2020). Even with highly accurate, high-resolution input data, river temperature models may fail to achieve this level of sensitivity due to boundary conditions and model parameterization (van Vliet et al., 2013; Wanders et al., 2019). Optimization is a prevalent strategy used in hydrologic modeling studies to mitigate errors in hydrological and land surface modeling research (Bonyadi & Michalewicz, 2017; Boussaïd et al., 2013; Cheng et al., 2023; Das et al., 2016; Tayfur, 2017). Nevertheless, the application of these techniques to river temperature models has remained relatively uncommon.

In this study, we create a chain of models to simulate river temperature in Alaskan rivers from 1990 to 2021. Our approach leverages the 4-km resolution RASM, which dynamically couples an atmospheric model with a land surface model specifically optimized to improve for cold region hydrology (Cheng et al., 2023). The model's process representation combined with its high resolution enables accurate representation of orographic effects, permafrost hydrology, and snow dynamics. River modeling utilized the river routing model, mizuRoute (Mizukami et al., 2016, 2022), in conjunction with the river temperature model, the River Basin Model (RBM, Yearsley, 2009, 2012). We conducted the first large-scale sensitivity analysis on RBM in Arctic regions to determine the most sensitive model parameters. We then optimized the model and compared it to a widely used statistical river temperature model for a benchmark to assess performance of our baseline and optimized physically based models, providing a more rigorous assessment of our model performance (e.g., Abramowitz, 2005; Best et al., 2015; Newman et al., 2017).

This approach, with its high-resolution climate input and comprehensive modeling framework, allows for an improved representation of the hydrological and thermal conditions occurring in the region as compared to the unoptimized and benchmark models. Notably, our model framework achieves highly accurate river temperatures from headwaters to mouth at high resolutions across the state reducing errors to within the thermal variability of

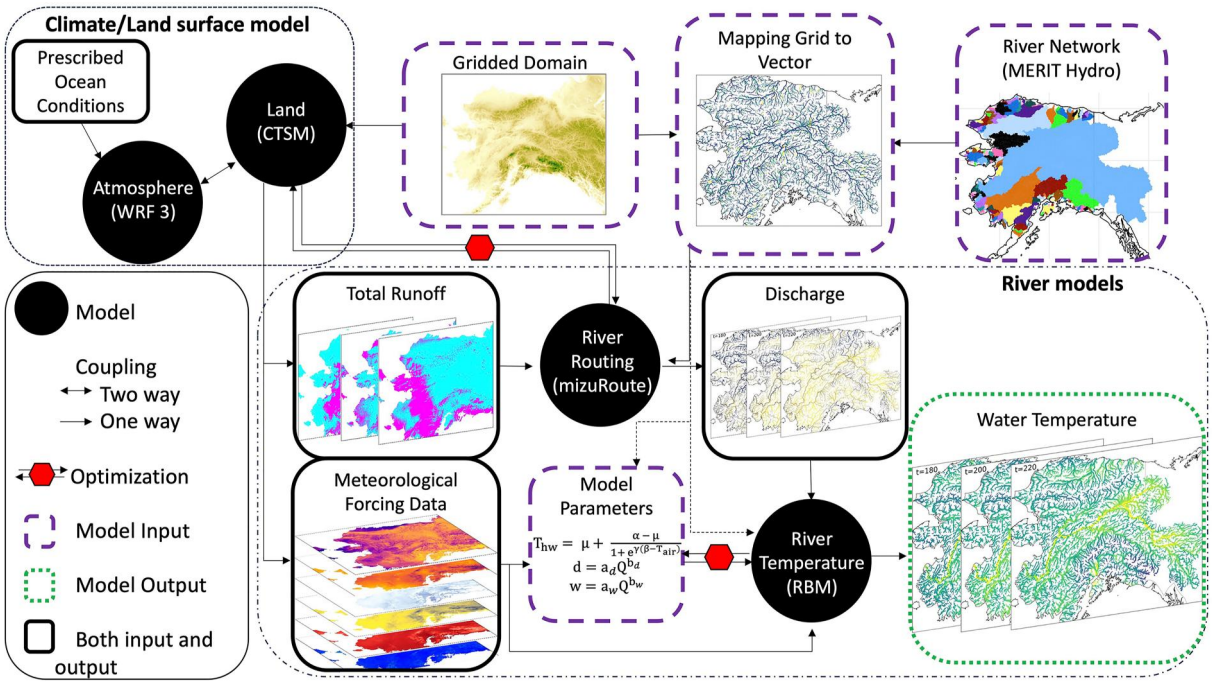

Figure 1. Flowchart of the chain of models and their interactions. While the water temperature regression is denoted as a separate model from the river temperature model, the River Basin Model includes a module to run the temperature regression to determine the headwater boundary conditions. The figure was adapted from Yearsley (2012, Figure 2).

fish species for the first time in regional modeling. The output from the modeling chain can provide the data necessary to understand the rapid changes in freshwater ecosystems that have occurred over the last 30 years (Oke et al., 2020).

2. Methods

Runoff from a coupled land-atmosphere RASM simulation was routed through mizuRoute to produce river discharge data. The discharge data along with the simulated meteorology from RASM were then used as input for RBM to simulate river temperature (Figure 1). Coupling of the river models was done "offline" meaning that each model was run completely before its output data were used as input in the subsequent model. The RBM was optimized using a Gaussian Process Regression surrogate model and the Non-dominated Sorting Genetic Algorithm II (NSGA-II, Deb et al., 2002) to generate model parameters. The optimized model system was run to simulate a 30-year historical period (1990–2021) for Alaskan rivers.

2.1. The Modeling System

2.1.1. Regional Arctic System Model (RASM)

We employed RASM, which dynamically couples the Weather Research and Forecasting (WRF, Skamarock et al., 2019) atmospheric model with the Community Terrestrial Systems Model (CTSM, Lawrence et al., 2019). Configuration of RASM for this regional application is described in more detail in Cheng et al. (2023). Notably, CTSM was optimized for streamflow and snow water equivalent in an offline manner and the optimized parameter set (Cheng et al., 2023) was subsequently used in RASM to generate a coupled, multi-decadal regional climate simulation. An iterative testing and re-optimization strategy was deployed to make sure the offline optimized parameters would not deteriorate the performance of the coupled models. Optimization for streamflow in a regional climate model is rare, and, to our knowledge, this is the first such effort in an Arctic region. Sub-daily hydrometeorological data were produced by RASM forced by downscaled ERA5 reanalysis for the domain for 1990–2021 at 4 km spatial resolution. Ocean and sea ice conditions were specified from ERA5 (Muñoz Sabater, 2019) to enhance the realism of Arctic weather simulations. Sub-daily data were temporally aggregated

to daily averages for use in the river models. While this specific model system was employed in our study, any regional or global model could serve as input to the river modeling system described here.

This is the first regional application using CTSM as the land component in RASM (Cheng et al., 2023). CTSM's distinctive features, such as explicit representation of frozen soil dynamics, complex vegetation and canopy representation, high resolution within the top 3 m of the soil layer, an adaptive time-stepping method for improved groundwater flow simulation, and a multi-layer snow model, contribute to a robust accounting of runoff generation in permafrost zones (Lawrence et al., 2019). Moreover, CTSM now includes a representative hillslope hydrology capability, enabling parameterization of slope and aspect impacts on lateral water transfer, incident radiation, and subsequent hydrological effects (Fan et al., 2019; Swenson et al., 2019). CTSM allows for ocean, lakes, glaciers, and mixed-use pixels correcting radiative effects over large bodies of water and ice, but neglects rivers, which is an adequate assumption at 4 km grid spacing. The land cover type was assumed to be static over the study period.

2.1.2. mizuRoute

mizuRoute is a stand-alone, vector-based, river routing model that calculates streamflow at each river segment. It employs a gamma-distribution-based unit hydrograph to simulate hillslope routing within a catchment and utilizes the impulse response unit hydrograph based on the Lohmann 1D diffusive wave approximation for river channel routing. mizuRoute requires two parameters for the impulse response function: wave velocity and diffusivity, but these have minimal impact on model performance (Mizukami et al., 2017). Total (gridded) runoff generated by CTSM is used as the only model input (Figure 1). Gridded input data were mapped to river segments using a weighted average of the watershed intersection with each grid cell. River channel information is obtained from MERIT Hydro (Yamazaki et al., 2019), which is described in Section 2.3.

2.1.3. The River Basin Model

The RBM is a physically based, one-dimensional, stream temperature model that was designed to operate on a grid (Yearsley, 2012), but has been modified in this study to operate on vectorized river segments. It solves the heat advection equation using a semi-Lagrangian approach (Yearsley, 2009, 2012). Water temperature is simulated by tracking water parcels through segments of the channel network then calculating the air-surface heat exchange and the heat advected from lateral inflows (Yearsley, 2009, 2012). At a given river segment, surface water and groundwater inputs are assumed to be at the same temperature and hyporheic exchange is neglected. RBM requires meteorological forcing data (air temperature, shortwave and longwave radiation, vapor pressure, atmospheric pressure, and wind velocity) at daily timesteps, which were obtained from RASM (Figure 1). The radiation terms account for topographic shading but do not consider vegetation shading at ground level. Vapor pressure deficit was output from RASM, so vapor pressure was calculated using the Clausius-Clapeyron relation (Clausius, 1850). The same procedure to map gridded data to vectors for mizuRoute was used in RBM. Meteorological variables were not adjusted for above stream conditions and could be a source of error within the model (Benyahya et al., 2010; Guenther et al., 2012; Leach & Moore, 2010). Vectorized river discharge output by mizuRoute was also used as an input to RBM. Additionally, the model requires boundary conditions at upstream boundaries and river channel geometry at each segment as determined through parameterization and described in Section 2.2. Since the model does not calculate river ice, a minimum water temperature was set to 0.1°C in the model.

2.1.4. Statistical Model

A commonly applied statistical model, which calculates river temperature using a non-linear equation that relates air temperature at the gage location to river temperature, was used as a benchmarking intercomparison to the physically based RBM. Model benchmarking is a technique widely used in land surface modeling. This technique uses a simplified model that has more flexibility to reproduce observed behavior to set performance expectations for more complex models before simulations are performed (Best et al., 2015; Newman et al., 2017). The non-linear statistical model proposed by Mohseni et al. (1998) is a computationally frugal way to simulate water temperature (Mantua et al., 2010; van Vliet et al., 2011). This statistical relationship is also the headwater boundary condition with RBM, and it is described in more detail in Section 2.2 (Yearsley, 2012). This statistical model is simplistic so it represents a minimum benchmark the physical model must achieve. The statistical model

underwent the same optimization workflow as RBM (described in Section 2.4) to determine the optimal set of Mohseni parameters. Both models used the same input air temperature. However, a universal parameter set was found to perform better in the statistical model than the regionalized parameters, so universal parameters were used.

2.2. Model Parameters

RBM has two sets of model parameters: Leopold parameters, used to determine channel geometry and flow velocity at every river segment, and Mohseni parameters used to determine river temperature at the headwaters (the most upstream river segments within the model), a boundary condition for the model.

Results from using Leopold parameters were compared to those using average river widths from the MERIT Hydro data set (Yamazaki et al., 2019), and Leopold parameters were found to improve the model performance of daily river temperatures. Additionally, the use of Leopold parameters outperformed the use of average river widths and discharge in Manning's equation (Manning et al., 1890) to calculate velocity and average water depth (results not shown). Leopold parameters come from a set of power law relationships used to relate discharge to channel geometry (Equations 1 and 2) established by Leopold and Maddock (1953):

$$d = a_d Q^{b_d} \tag{1}$$

$$w = a_w Q^{b_w} \tag{2}$$

where, d is the average river depth, w is the average river width, Q is the daily averaged instantaneous discharge, and a_d, b_d, a_w, and b_w represent the Leopold parameters that establish a statistical relationship between discharge and river width (parameters subscripted with w) and average depth (parameters subscripted with d). The average water velocity for each segment is calculated using the continuity equation (Equation 3).

$$u = \frac{Q}{d \times w} \tag{3}$$

When discharge is near 0 $m^3\ s^{-1}$, the Leopold parameters can result in near zero river width, depth, and velocity, so minimum values of these parameters are set to ensure model stability (Cheng et al., 2020). Since these are prescribed limits, they were added to the optimization. The model utilizes a statistical relationship between air temperature (T_{air}) and the water temperature (T_{hw}) for the upstream boundary condition at the headwaters (Equation 4) (Mohseni et al., 1998; Yearsley, 2012).

$$T_{\text{hw}} = \mu + \frac{\alpha - \mu}{1 + e^{\gamma(\beta - T_{\text{air}})}} \tag{4}$$

where μ = lower bound of water temperature (°C) (i.e., as air temperature decreases, the water temperature will not be able to decrease below the value set for μ), α = upper bound of water temperature (°C) (i.e., as air temperature increases, the water temperature will not be able to increase above the value set for α), γ = steepest slope of the air-water temperature relationship function, and β = air temperature (°C) where γ occurs.

These collectively make up the Mohseni parameters. Therefore, a total of 11 parameters (four Leopold parameters, three minimums, and four Mohseni parameters) were analyzed to determine their impact on overall performance.

van Vliet et al. (2012) added a lag effect to the temperature regression, because water temperatures often lag air temperatures on daily time scales.

$$T_{\text{smooth}} = (1 - \lambda)\, T_{\text{air}}(t - 1) + \lambda T_{\text{air}}(t) \tag{5}$$

where T_{smooth} is the weighted average air temperature of the current (t) and previous ($t - 1$) time step, and λ is the lag coefficient. When observational data are fitted with this equation, the lag parameter was found to be generally constant at 0.1 (van Vliet et al., 2012), so this parameter was not optimized.

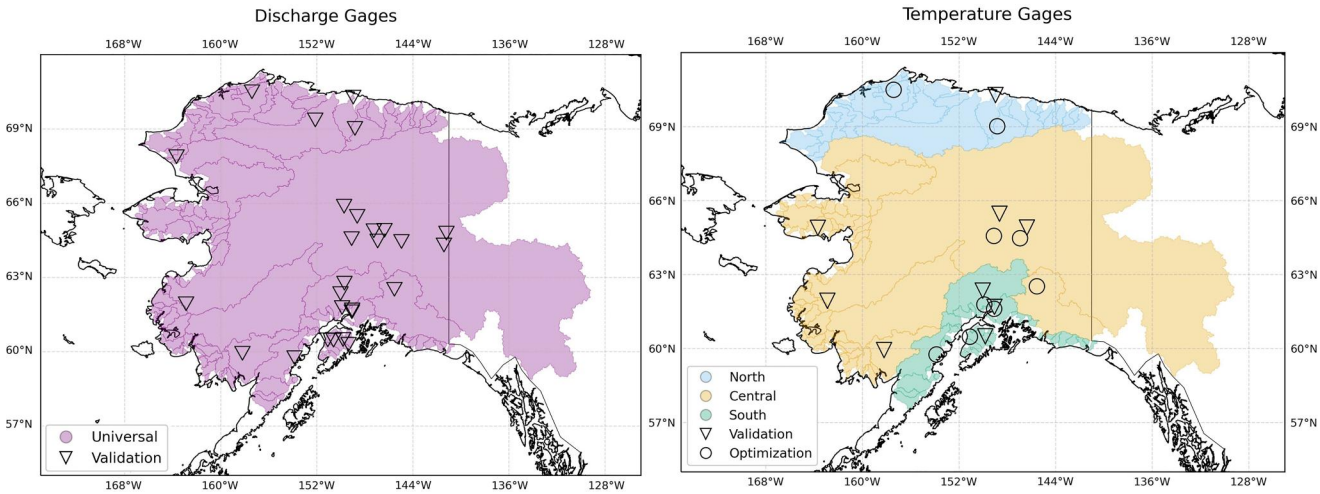

Figure 2. Data availability used in the optimization and validation of mizuRoute (Mizukami et al., 2022) and River Basin Model (Yearsley, 2009, 2012). U.S. Geological Survey gages from the National Water Information System (U.S. Geological Survey, 2022) are plotted by how the data were used. Each river basin in the study area is shaded by the regional or universal parameter sets used in modeling.

2.3. Data

River basins and channel locations, extending to small first-order streams, were determined based on the MERIT Hydro data set (Yamazaki et al., 2019). In this data set, a river basin is defined by its outlet to the ocean, so there is only one outlet per basin. Included in this study are river basins with outlets in the state of Alaska, excluding the Aleutian Islands and Southeastern Alaska. To filter out the small coastal streams, only river basins with at least 10 hydrological response units (HRUs) were retained. These criteria were met by 138 unique river basins across Alaska (Figure 2), comprising more than 34,000 HRUs.

Observed river temperature and discharge data were obtained from the United States Geological Survey (USGS) National Water Information System (U.S. Geological Survey, 2022). Only gages with more than 8 years of data between 2013 and 2021 were used for model optimization and validation. Only river discharge data that were 90% complete over this period were included resulting in 27 gages used for validation (Figure 2). Availability of river temperature data is less consistent, so each gage that covered this period was visually inspected for completeness resulting in 18 gages used for optimization and validation (Figure 2). Both river temperature and discharge data are quality controlled by the USGS before they are published (Wagner et al., 2006). Only one gage had a complete set of temperature data for the period but did not have complete discharge data. Gage information is provided in Table S1.

A range of Mohseni parameters was developed by comparing USGS river temperature data for ice-free months from gages that had less than 100 km^2 of contributing area to near surface air temperature data produced by the climate model (Table 1). Field notes from USGS river gage technicians were used to establish a range of Leopold parameters and channel geometry (Table 1). Discharge, velocity, and river width were reported, and the average depth was calculated using the continuity equation. All USGS data were accessed using the dataRetrieval package in R Statistical Software v4.2.1 (DeCicco et al., 2023; R Core Team, 2022).

Regional differences in these parameters were observed, resulting in the model being divided into three regions: North, Central, and South (Figure 2). The regional boundaries were based on the hydrologic regions of Alaska as determined by the USGS but were further constrained by data availability. Of the 18 gages, nine were randomly selected using a random number generator to serve as optimization, ensuring at least two optimization gages in each region, and the other nine were reserved for validation (Figure 2). A baseline model was run using the median value of each of these parameters for each region.

2.4. Optimization

A computationally efficient optimization method based on surrogate modeling, which has been applied to other hydrologic models (Cheng et al., 2023; Gong et al., 2016; Wang et al., 2014), was used to optimize RBM

Table 1
The Parameter Range of Model Parameters as Determined by U.S. Geological Survey Field Data of Alaskan Rivers From the National Water Information System (U.S. Geological Survey, 2022), Which Were Used in Model Optimization

Variable	Min	Max	Median	Mean
α	8.77	16.54	11.68	11.79
β	6.36	14.96	9.07	9.4
μ	−0.23	3.1	−0.02	0.42
γ	0.17	0.48	0.38	0.33
a_d	0.045	2.42	0.11	0.19
b_d	0.14	0.64	0.34	0.35
a_w	2.2	383.5	9.5	33.6
b_w	0.05	0.54	0.21	0.23
Minimum velocity (m/s)	0.02	1.03	0.26	0.31
Minimum depth (m)	0.03	11.58	0.21	0.60
Minimum width (m)	0.91	670	12.7	53.3

parameters. The optimization was performed based on the workflow established by Cheng et al. (2023), which detailed the optimization of the land surface model used in the model system described here. In the current study, we perform the optimization of the river temperature model. Instead of the Nash-Sutcliffe Efficiency, we used the Root Mean Square Error (RMSE) of mean daily stream temperature as the objective function, which is more common in river temperature analysis. Initially, 200 parameter combinations were sampled using the Latin Hyper Square (LHS, McKay et al., 2000) method across the parameter space, and the objective function was calculated for each combination.

After the initial sampling, the rivers were separated into the three regions. A Gaussian Process Regression model was trained as a surrogate model to determine the response of the objective function across the parameter space for each region. The Non-dominated Sorting Genetic Algorithm II (NSGA-II, Deb et al., 2002) was then employed on the surrogate model to sample 20 new optimal parameter sets for each region in the next iteration. Each iteration utilized all samples from the initial sampling and all previous iterations of that region to train a new surrogate model. Iterations were stopped when there was minimal improvement in model performance. In total, 20 iterations were conducted, resulting in 600 samples for each region. *K*-fold cross-validation ($k = 5$) was employed to assess the accuracy of the surrogate model, comparing the RMSE of the simulated objectives from the surrogate model with the objectives calculated from RBM results.

The optimization was performed using data for years 2014–2017. 1 January 2013 to 30 April 2014, was used as the spin-up period for the model. Given that river water temperature resets close to 0°C each winter, a relatively short spin-up time was sufficient for this model. The optimization was conducted only for ice-free months: May–September for the South and Central regions, and June–September for the North. This difference is due to later ice breakup in the North.

2.5. Sensitivity Analysis

The model was evaluated for its sensitivity to input air temperature and discharge. The model was run multiple times, perturbing each input. Temperature was adjusted by −2, −1, 1, and 2°C and the modeled error of average daily river temperature and maximum seasonal river temperature per degree change in air temperature was evaluated. Similarly, discharge was varied using 80%, 90%, 110%, and 120% of discharge, and the modeled river temperature error per 10% change in discharge was evaluated.

The sensitivity of model parameters was assessed using the surrogate model. After all iterations, the surrogate model was used to determine the response of the objective function to each parameter. By fixing all other parameters at their median values and varying only the target parameter, a two-dimensional response curve for each parameter was generated. The difference between the maximum and minimum error of the response curve was used as the error factor for each parameter, with higher values indicating a greater change in the model error as a result of adjusting the parameter.

2.6. Validation and Production

mizuRoute was validated against discharge data from 27 USGS gage locations for 8 years spanning 2013–2021 (U.S. Geological Survey, 2022). The Kling-Gupta Efficiency (KGE, Gupta et al., 2009) was used as the objective function on mean daily streamflow. This metric includes linear correlation, flow variability error, and bias. The validation was performed on ice free months (May–September).

RBM was validated against data from 18 USGS gages for the years 2018–2021 (U.S. Geological Survey, 2022) found in Table S1. 1 January 2017 to 30 April 2018 was used as the spin-up period for the model. The RMSE was used as the objective function, assessing daily temperature data for ice-free months. The optimized parameter values were compared to the baseline parameter values and the statistical model. A model outperformed another model when it had a lower RMSE, which can occur based on different parameter sets used in the model validation.

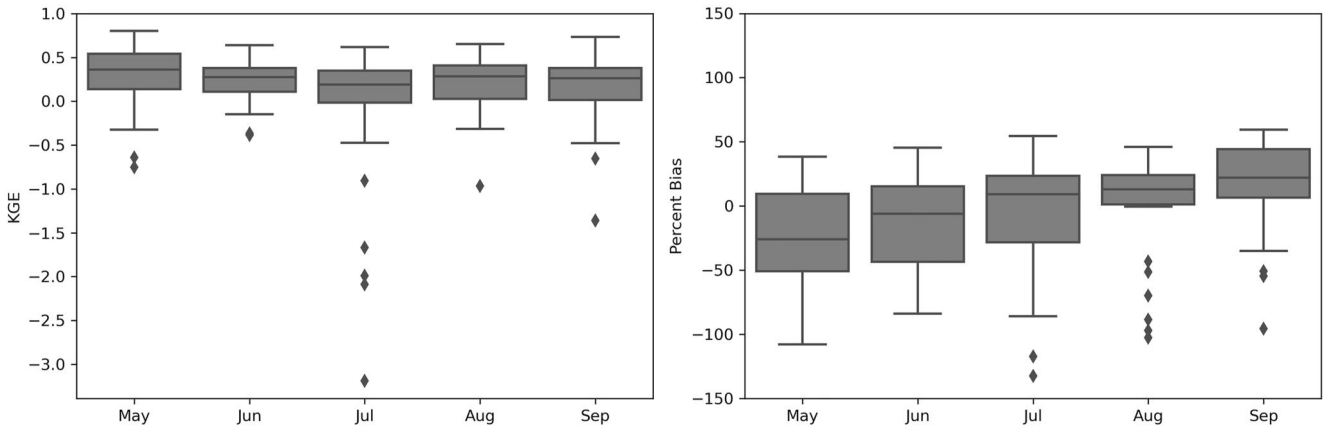

Figure 3. The validation of the mizuRoute by month (Mizukami et al., 2022). Left: The Kling-Gupta Efficiency of discharge during ice free months, May–September, at 27 U.S. Geological Survey gages from the National Water Information System (U.S. Geological Survey, 2022) for water years 2013–2021. Right: The percent bias at those gages.

Daily river discharge and river temperature values were simulated for all 138 basins for 1 January 1990 to 30 September 2021. Each basin was run using the optimized parameter set for the region. The basins were separated into their geographic region by their outlet point (Figure 2). While the river routing model was not directly optimized, the runoff produced by the land surface model CTSM was previously routed and optimized against USGS discharge observations for selected basins in Alaska (Cheng et al., 2023; Lawrence et al., 2019). All modeling was conducted on the NCAR Cheyenne supercomputer (Computational and Information Systems Laboratory, 2019).

3. Results

3.1. River Routing Validation

The median KGE calculated for daily discharge using the validation gages across the full study domain was 0.45 for the ice-free months and a KGE of 0.47 with a percent bias of −4.6% annually. The results are shown spatially in Figure S1 in Supporting Information S1. When assessed by month, May had the highest median KGE (0.36) and July had the lowest (0.19) (Figure 3). The percent bias shifted seasonally from a median negative bias in May (underestimating discharge by 26%) to a median positive bias in September (overestimating discharge by 22%) (Figure 3).

3.2. River Temperature Model Validation

The river temperature optimization process required 20 iterations (600 total model runs) to produce the optimized parameter values (Table S2 in Supporting Information S1). The surrogate model RMSE was 0.78°C. Overall, the optimization improved the RMSE of RBM from 3.24 to 2.04°C during the validation period, with a range of 1.10–3.18°C. After optimization, river temperature simulations were substantially improved in all three regions (Table 2). The Central region exhibited the most improvement, while the South region had the lowest overall error. Among the gages used for optimization, the model performance improved in eight of the nine gages, resulting in an average decrease from 3.27 to 1.78°C. Additionally, the optimization improved temperature simulations at six of nine gages that were not used in the optimization decreasing the average RMSE from 3.20 to 2.31°C. All three gages located in different river basins than the optimization points showed substantial performance improvements with optimization, reducing the average RMSE from 4.72 to 2.18°C.

Table 2
Validation Root Mean Square Error (RMSE) of Optimized and Baseline RBM (Yearsley, 2009, 2012) Parameter Values During Ice Free Months, May–September, at 18 U.S. Geological Survey Gages From the National Water Information System (U.S. Geological Survey, 2022) for Water Years 2018–2021 for the Three Regions Within the Study

Scenarios	North (n = 3)	Central (n = 8)	South (n = 7)
Baseline RMSE (°C)	3.15	4.34	2.01
Optimized RMSE (°C)	2.25	2.31	1.65

The optimized model was compared to the baseline model and a benchmark statistical model (Figure 4). The statistical model had an optimization RMSE of 2.2°C and a validation RMSE of 2.97°C. At >75% of the gages, the optimized model outperformed both the statistical model (15 of 18 gages) and

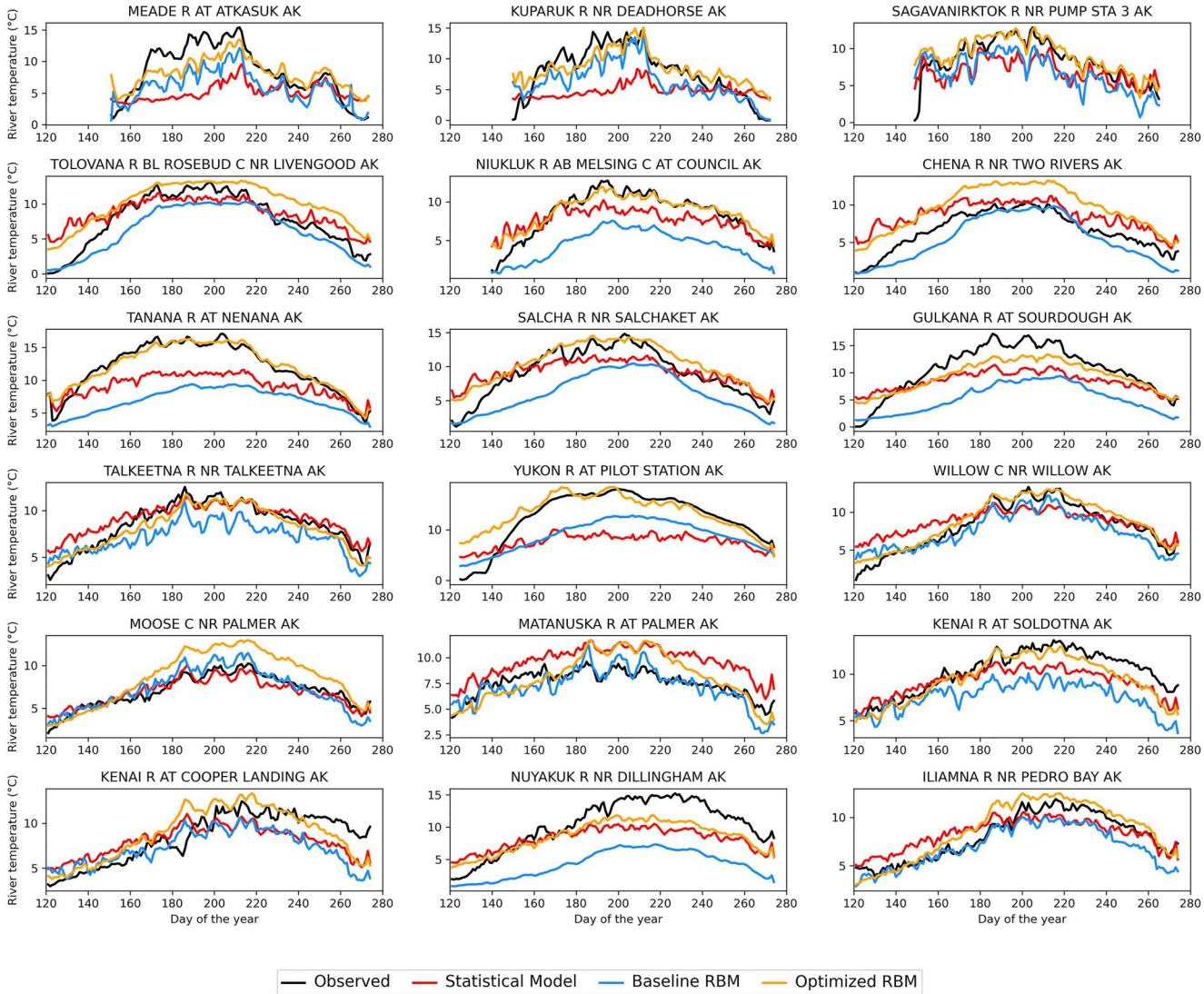

Figure 4. Average modeled values by day of the calendar year during the validation period for the benchmark statistical model and River Basin Model run with optimized parameters and baseline parameter values. Rivers are arranged north to south and are named according to the U.S. Geological Survey National Water Information System (U.S. Geological Survey, 2022).

the baseline model (14 of 18 gages). At the three locations where the statistical and baseline models both outperformed the optimized model, the baseline model had better temperature simulations than the statistical model at two. However, the benchmark statistical model outperformed the baseline model at half of the 18 gages. The statistical model performed well in the South and Central basins, excluding the Yukon River (RMSE of 6.33°C), but poorly in two of the three North basins (RMSE of 4.5°C).

Monthly RMSE analysis demonstrates that the optimized river temperature model consistently outperforms the baseline conditions and the statistical benchmark model throughout the ice-free period (Figure 5). In the optimized model, the highest error occurred in May (2.81°C) and the lowest error in September (1.67°C). Rivers in the South region show greater variability in error across months, ranging from 1.06 to 2.19°C, respectively, while the North and Central regions display more consistency. The South performs better in spring and fall, with the highest error occurring in July. The North and Central regions exhibit more varied performance, with the North performing best in August and worst in June, while the Central region shows the best performance in September and the worst in May. Unlike the South, which has its lowest errors in May and September, the Central region only has notably lower error in September.

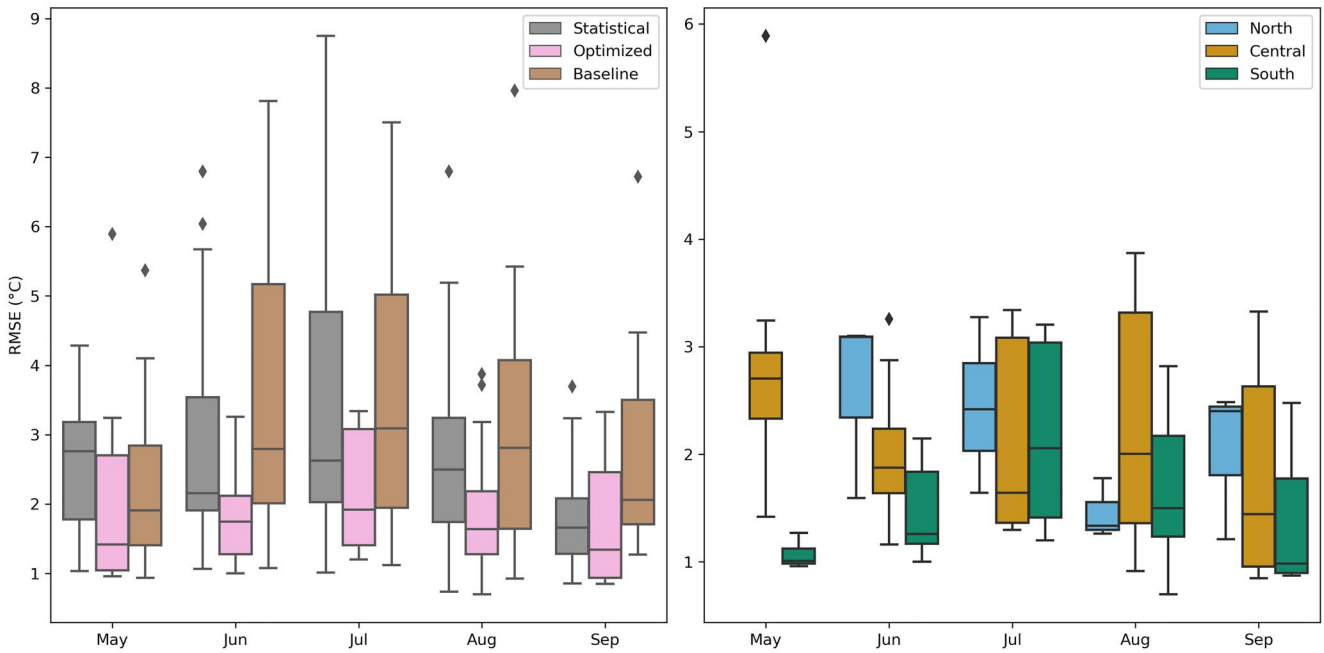

Figure 5. Left: the optimized River Basin Model versus baseline parameters and the benchmark statistical model by month during ice free months, May–September, at 18 U.S. Geological Survey gages from the National Water Information System (U.S. Geological Survey, 2022) for water years 2018–2021. Right: optimized model performance by month and region during the validation.

Simulated daily river temperature data from the optimized RBM are plotted against daily observations to illustrate model performance, along with the histogram of the error (Figure 6) by month and throughout the ice-free period. The model struggles to capture low river temperatures, as inferred from the clustering of points above the 1:1 line on the left side of each graph (Figure 6). In May, some rivers still contain ice, keeping the river temperatures close to 0°C, while the model predicts higher temperatures. This results in a slight warm bias in the model. The mean overall difference between simulated and observed river temperatures is 0.46°C (range 0.28–0.96°C by month), with a standard deviation of 2.08°C (range 1.81–2.34°C by month).

In the optimized model, there was significant variation within the regions. For example, two rivers in the Central region, the Chena and Tanana, did not share a set of parameters that increased model performance for both rivers, each river performed better at the other gage's expense. The optimized parameter values for the Central region produced a better fit for the Tanana River and a worse fit in the Chena River, causing it to underperform against the benchmark (Figure 7). The validation of the optimized model is shown spatially in Figure S2 in Supporting Information S1. Model performance also varied by river size. There was only one first order stream in the validation set, which underperformed the statistical model (RMSE of 1.18 vs. 2.22°C). There was an optimization gage with a slightly higher RMSE (1.87°C) on a fourth order river downstream of this first order stream gage. A second order stream was an optimization point in a basin with a fourth order stream validation point, resulting in similar performance (1.14 and 1.10°C, respectively). The seventh order lower Yukon River is the largest river in the data set. At this gage, the optimized model performed well (RMSE of 2.69°C), where the benchmark model had its worst performance (RMSE of 6.33°C).

3.3. RBM Sensitivity Analysis

The average daily temperature error of the optimized RBM changes 0.31 per 1°C change in air temperature and the maximum seasonal temperature error changes 0.88 per 1°C in air temperature. Changes in discharge resulted in an average error change of 0.01°C per 10% change in discharge for daily averaged water temperatures and 0.09°C per 10% change in discharge for seasonal maximum water temperature.

Parameter sensitivity was obtained from the surrogate model. The only consistently sensitive parameter was μ (Figure 7), the lower bound of calculated water temperature for the boundary condition, which resulted in the

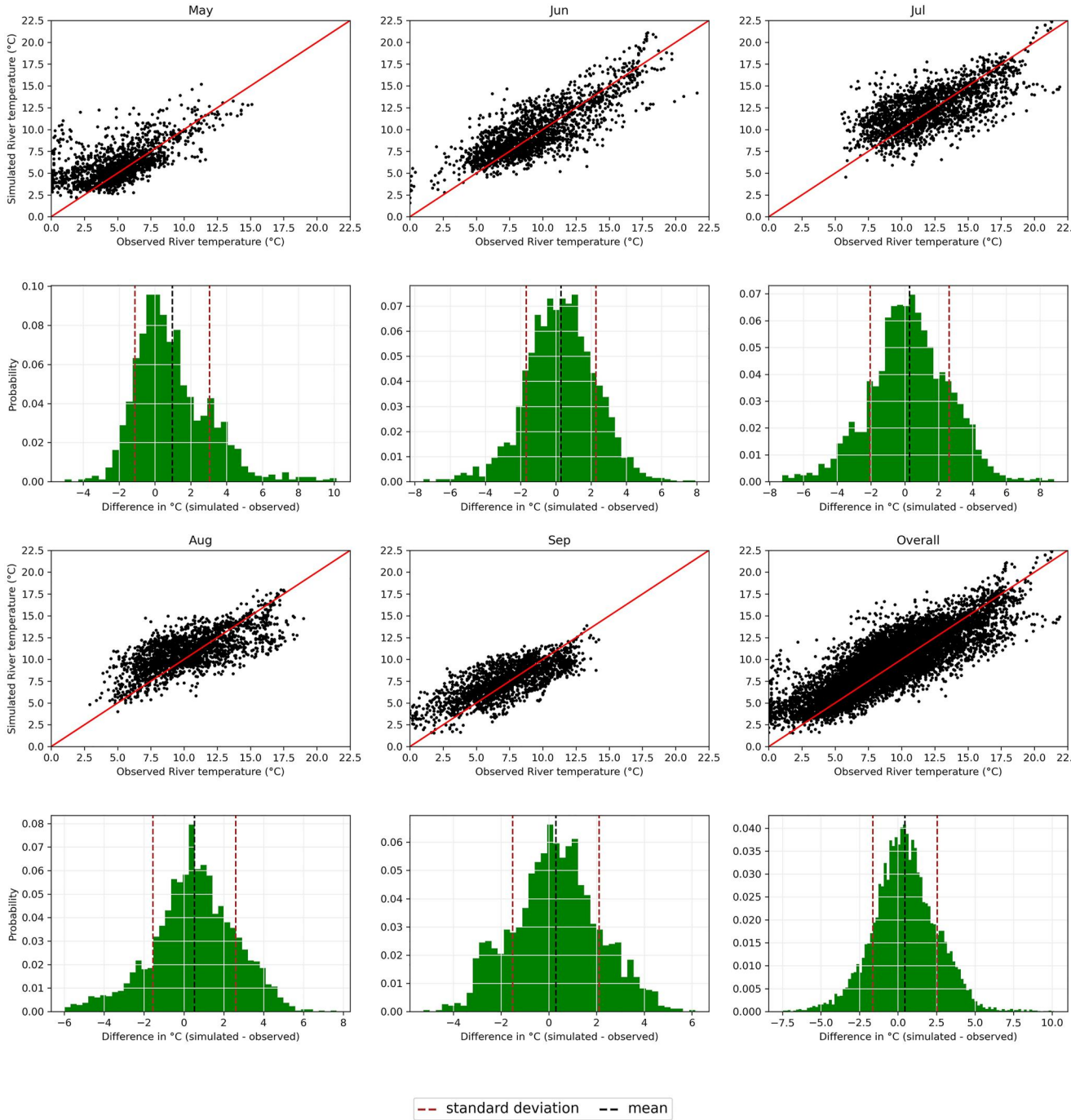

Figure 6. Scatter plots of simulated versus observed daily temperature values and bar plots of the error probability for the validation of River Basin Model during ice free months, May–September and overall, at 18 U.S. Geological Survey gages from the National Water Information System (U.S. Geological Survey, 2022) for water years 2018–2021. The mean and standard deviation of model error are also plotted on the bar plots.

largest range of model error. The minimum depth was among the least sensitive parameters in the South and Central regions, but it ranked as the third most sensitive parameter in the North. In the North and Central regions, β and b_w were the least sensitive parameters, while they were the fourth and second most sensitive parameters in the South, respectively.

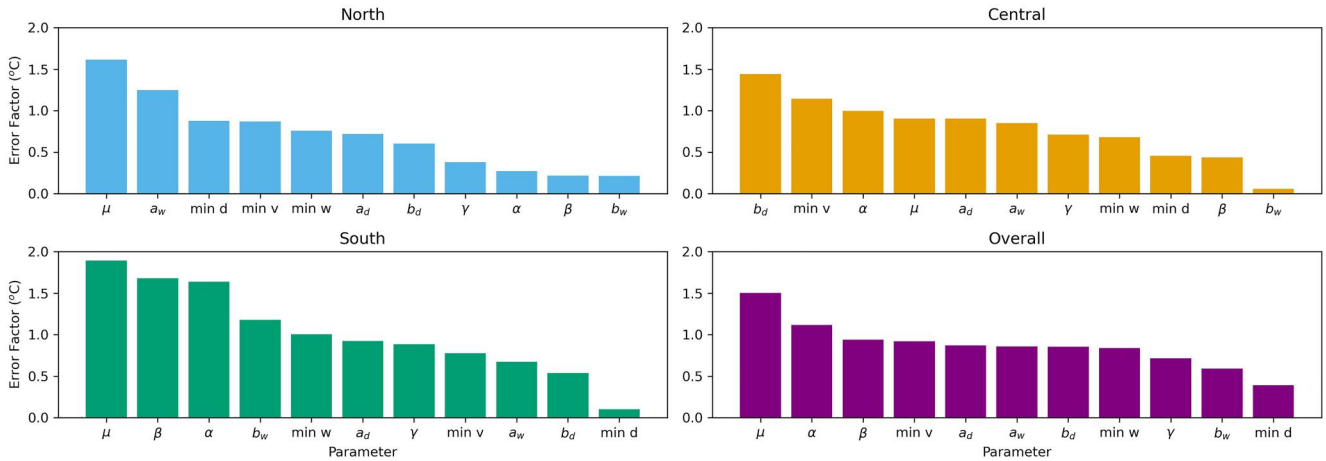

Figure 7. The error factor of each parameter, defined as the amplitude of the response curve after the last iteration of the optimization, by location and overall.

3.4. High Resolution River Temperature Simulation

The model was run with the optimized regional parameter sets for 138 basins across Alaska and the Yukon River basin to generate a continuous river temperature hindcast from 1 January 1990 to 30 September 2021. The model was only optimized and validated for the ice-free months. The mean river temperature across Alaska during the ice-free months was 8.3°C (Figure 8). The average maximum temperature was 14.3°C, the minimum was 1.7°C, and the variance was 8.2°C^2. Rivers in the North region had higher maximum temperatures (16.5°C) compared to the Central and South regions (14.0 and 13.6°C, respectively), which is similar to observed data at USGS gages (Figure S3 in Supporting Information S1). The lowest maximum temperatures occurred in headwater streams (13.7°C). The Central Region had the highest mean water temperature (8.5°C).

4. Discussion

By utilizing the RASM at 4-km resolution, optimizing both land surface and river temperature models, and conducting the first large-scale sensitivity analysis of the RBM in the Arctic, we successfully generated a highly accurate, high-resolution hindcast of river discharge and temperature for 138 basins across Alaska. The model optimization proved effective, reducing error below the baseline and statistical benchmark model, highlighting the success of this optimization strategy. Furthermore, the benchmark statistical model exhibited superior performance over baseline parameter values in RBM, emphasizing the utility of applying only optimized physical models rather than "default" parameters taken from the literature and applied to this region. Notably, the simplified statistical model may be adequate for modeling smaller streams with limited advective influences and limited shallow groundwater inputs due to permafrost.

Modeling Arctic river temperatures presents challenges due to snowmelt-driven peak discharge coinciding with the highest annual water temperatures, altering the relationship between water and air temperatures (van Vliet et al., 2011). In Alaska, shortwave radiation and air temperature have been identified as the dominant influences on river temperatures, justifying the adoption of RBM—a model expressly designed to accommodate these processes (Chikita et al., 2010; King & Neilson, 2019; Yearsley, 2009). Additionally, high-resolution modeling using atmospheric and land surface models specifically designed for snowmelt runoff in permafrost zones may help to capture this dynamic. Moreover, hyporheic exchange during low flows, a phenomenon not explicitly addressed in RBM, has been demonstrated to affect Arctic river temperatures (Cozzetto et al., 2013; King & Neilson, 2019; Yearsley, 2009). Given that the lowest flows in the model coincide with the boundaries where river temperatures are prescribed, the model optimization inherently considers and accounts for this process.

Statistical and physical models have been employed to understand river temperatures in the Arctic, ranging from reach-scale to global simulations. Whereas reach-scale estimates can achieve a high degree of accuracy (RMSE <1°C), global simulations often struggle to accurately represent the Arctic region (RMSE >4°C) (Chikita et al., 2010; King & Neilson, 2019; Wanders et al., 2019). Although regional applications of river temperature

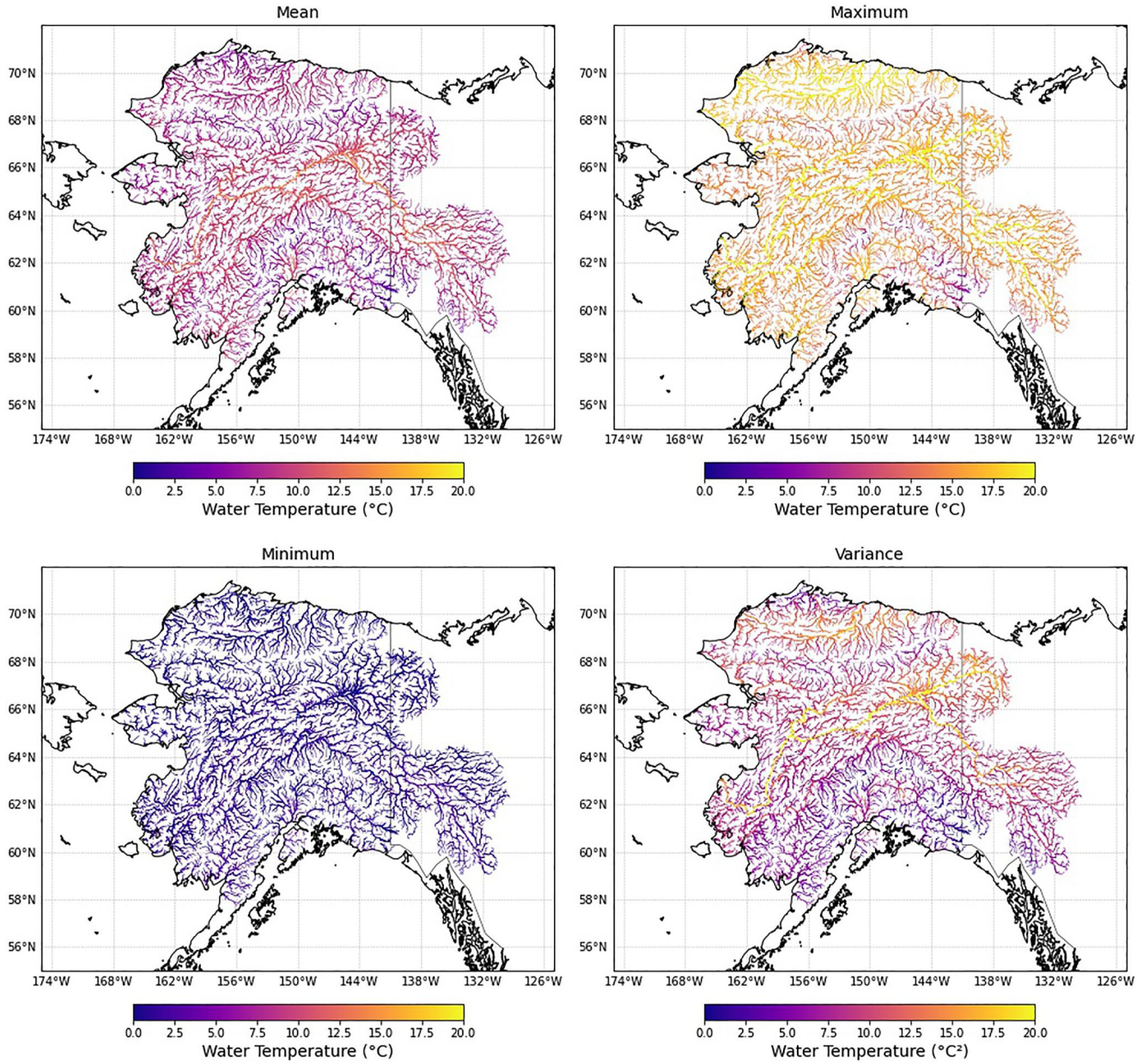

Figure 8. Mean, maximum, minimum, and variance in water temperature average over the ice-free months, May–September, for the period 1990–2021. River segments are sized by stream order and first order streams are not shown.

models in the Arctic are rare, numerous studies have been conducted in the contiguous United States, where river temperature modeling is generally more accurate with global models achieving RMSE of around 2.5°C (Isaak et al., 2017; Niemeyer et al., 2018; van Vliet et al., 2012; Wanders et al., 2019). Our modeling system met and surpassed the mean error achieved by these regional models despite the complex Arctic hydrology. The resulting comprehensive framework, incorporating high-resolution climate data from a regional climate and land surface model that has been calibrated on snowpack and discharge observations, establishes a new standard for accurately simulating river temperatures in Arctic rivers. Our results surpass previous model skill metrics and provide critical insights into the dynamic changes in freshwater ecosystems over the past three decades (Cheng et al., 2023; Niemeyer et al., 2018; van Vliet et al., 2012, 2013; Wanders et al., 2019; Yearsley, 2012).

4.1. Regional Difference in Model Parameters and Outputs

In the North, rivers are simulated to have the highest maximum river temperatures. The underperformance of the benchmark statistical model in the North suggests that air temperature is not the dominant influencer of river temperature. Rather, water temperature in Northern rivers is primarily shaped by incoming shortwave and longwave radiation (Zheng et al., 2019), a phenomenon aptly captured by RBM. Notably, the North region displayed greater sensitivity to Leopold parameters related to river geometry, impacting water velocity and the river's thermal sink capacity (Leach et al., 2023). The shallower Northern rivers can experience significant warming due to radiation, exceeding air temperatures (Cozzetto et al., 2006; Zheng et al., 2019). The presence of continuous permafrost underlying Northern rivers also keeps groundwater close to the surface, resulting in the warming of headwater streams (Sjöberg et al., 2021).

Conversely, high elevation streams in the South had the lowest simulated maximum water temperatures. In this region, the prevalence of late snowmelt runoff and glacial melt contributes to consistently cooler stream temperatures even as air temperatures rise during the summer (Bieniek et al., 2014; Brown & Hannah, 2008; Crossman et al., 2013; Curran & Biles, 2021). Although air temperature typically correlates with river temperature, this relationship breaks down in snowmelt and glacier-dominated areas potentially leading to overestimations in modeled stream temperatures (Ferchichi & St-Hilaire, 2023; Ficklin et al., 2012; Yan et al., 2021). Additionally, the shorter length of South region rivers, as compared to those in the North and Central regions, allows headwater boundary conditions to propagate extensively (van Vliet et al., 2012), possibly contributing to the pronounced influence of the boundary condition in this region. The Mohseni equation parameters used in the boundary condition, which indirectly factors in these dynamics through its non-linear formulation (Mohseni et al., 1998), were the most sensitive parameters in South's river temperature modeling.

Across all three regions, the Mohseni parameter μ, representing the lower bound of the headwater boundary temperature, emerged as the most sensitive parameter. While theoretically, this value should be 0°C, local conditions such as groundwater inputs, runoff, lake and reservoir effects, and solar radiation can maintain river segments above freezing even as air temperatures drop below 0°C (Mohseni et al., 1998). Since model optimization was conducted for the ice-free months the optimized value of μ was always greater than 0°C.

4.2. Importance of Model Structure, Parameterization, and Forcing Data

There are three major sources of error within RBM: model structure, parameterization, and forcing data. RBM only solves surface energy fluxes and advection. The one-dimensional nature of the model also neglects thermal gradients within the water column. Groundwater and hyporheic exchange are major controls on river temperatures that are not directly considered in RBM. In northern Alaska, shallow, suprapermafrost groundwater warms streams, while in other areas not underlain by continuous permafrost, groundwater will cool streams (Leach & Moore, 2019; Sjöberg et al., 2021). In first order streams, groundwater is the primary driver of water temperature, but this is also where the boundary conditions exhibit the greatest influence in RBM (Caissie, 2006; van Vliet et al., 2013). The Mohseni equation indirectly accounts for groundwater input affecting river temperature through its non-linearity (Mohseni et al., 1998). Furthermore, our river modeling system does not explicitly consider the thermal regulation of lakes, which has limited local effects at regional scales (Isaak et al., 2017). Instead, it relies on the Mohseni equation at the upstream boundary to account for this thermal regulation (Mohseni et al., 1998). Given that air temperature and shortwave radiation are the primary drivers of river temperature, the most significant source of error not addressed in the model is the meteorological difference between the grid cell and the air-water interface (Chikita et al., 2010; Guenther et al., 2012).

The model parameterizes channel geometry and the headwater boundary condition, which can lead to errors since river temperature models are sensitive to parameterization (Piotrowski & Napiorkowski, 2018). Our model, operating on a high-resolution river network, will consistently have headwater streams flowing into the main channel influencing river temperature, so the boundary conditions are highly influential (van Vliet et al., 2013), which differs from the modeling of small river segments (Wondzell et al., 2019). Our sensitivity analysis shows that parameterization, especially of the boundary conditions, is the primary error within the model.

Parameterization of the boundary conditions and channel geometry was conducted over three geographical regions, but there was significant variability within those regions. For example, two rivers in the Central region did not share an optimal set of parameters despite their proximity. One river is characterized by its substantial size,

braided morphology, higher discharge, and glacial influence, whereas the other is a smaller, meandering river, devoid of glacial influence, that experiences thermal pollution from human activities (Curran & Biles, 2021). This indicates that geography is not the only factor affecting model parameter choice. Other hydrologic features such as glaciers and snowmelt can also affect the headwater boundary conditions (Yan et al., 2021). These variables as well as elevation and river morphology were explored as alternatives to the geography-based separation of parameters, but there are only a limited number of USGS river temperature gages in headwater streams, which prevented separating river segments based on these variables. More long-term data and analysis may improve understanding of the effect that optimization across these variables would have on model performance.

River size may also be a factor in the model parameterization. The optimization gages encompass rivers ranging from second through fifth order, and over half of the optimization gages are in fourth order rivers. These rivers are usually larger and warmer than the headwaters as radiation and advection become the primary drivers of temperature (Fabris et al., 2020). It is within this range of river sizes that the model consistently displayed its optimal performance. In headwater streams, the model showed mixed results. In the sole first order stream used in validation, the model underperformed the benchmark statistical model, but still performs similar to average values of other river temperature models (van Vliet et al., 2013; Wanders et al., 2019). For the two available second order streams used as optimization points, both demonstrated superior performance compared to the benchmark model. In contrast, the Yukon River, classified as a seventh-order river, exceeded the largest optimization gage in the region by two stream orders, yet it yielded highly promising results, affirming the model's applicability to larger rivers. The performance disparity between the optimized model and the benchmark underscores the pivotal role of advection in influencing the thermal dynamics of these larger rivers. Such a finding also indicates the accuracy of upstream river temperatures in the simulation, as inaccuracies introduced in the upstream segments have the potential to magnify downstream.

Forcing data from the climate and land surface model represent the last major source of error within the model. Biases in the input data could propagate through the model chain, which might not be compensated by the parameter optimization. van Vliet et al. (2012) demonstrated that errors in discharge of 50% could result in significantly different errors within RBM for maximum water temperatures. We found similar changes in error in response to perturbing discharge. We also evaluated air temperature and found that it had a much larger impact on model error than river discharge. This aligns with field studies of river temperature that have concluded that solar inputs and air temperature were the primary drivers of river temperature (Bolduc & Lamoureux, 2018), while discharge has a minor effect after a certain minimum flow is reached (Cheng et al., 2020; Gu et al., 1998). This suggests why the errors in the river routing model (mean KGE = 0.46) do not significantly affect the river temperature model.

4.3. Modeled River Temperatures and Fish Health

River temperature models are vital to assess thermal regimes in rivers, particularly for fish and other aquatic organisms whose physiological processes are influenced by water temperature (Durance & Ormerod, 2009; Pörtner & Farrell, 2008). Organisms thrive within specific temperature ranges, but these bounds can vary by as much as 2–3°C within species at the same life stage in the same river, and even more significantly over larger geographical regions (Coutant, 1999; Pörtner & Farrell, 2008). Before optimization, RBM performance fell outside the range of natural variability within species. However, after optimizing the model, the error decreased to 2.04°C, indicating that it now aligns with the natural fluctuation of suitable conditions and thus is appropriate for addressing questions related to the impact of river temperature on fish health. This demonstrates the effectiveness of the offline coupling of mizuRoute and RBM, as well as the optimization workflow, in accurately simulating river discharge and temperature using inputs generated by a regional climate model. Such modeling efforts support understanding the impact of climate change on fish species and provide valuable insights into thermal thresholds within and across rivers.

5. Conclusions

Our study presents the first high-resolution river discharge and temperature hindcast for rivers in Alaska and the Yukon River basin from 1990 to 2021, utilizing a novel coupling of mizuRoute and RBM forced by a 4 km regional climate model and land surface model. The sensitivity analysis conducted on RBM underlines the critical importance of precise input data, particularly air temperature data, and parameter optimization. Our surrogate

model optimization strategy proved to be highly computationally efficient and yielded substantial improvements in modeled performance relative to the baseline model. Notably, while a benchmark statistical river temperature model outperformed the unoptimized RBM at more than half of the gages, it underperformed in comparison to the optimized RBM, thereby emphasizing the pivotal role of model optimization. The regional variations in model performance strongly highlight the need for tailored approaches that consider local conditions. The sensitivity analysis indicates important drivers of river temperatures in each region and how they differ across the state. Ultimately, the comprehensive river discharge and temperature hindcast provides an invaluable resource for gaining insights into long-term river temperature patterns. For instance, the findings reveal that northern rivers exhibit the highest maximum water temperatures and display the greatest variability throughout the study period, which is consistent with observations. These river temperature fluctuations can have significant ecological implications for freshwater ecosystems, which will continue to be altered by a changing climate. The hindcast data can potentially be applied to ecological assessment, policy development, and climate change research.

Data Availability Statement

mizuRoute (Mizukami et al., 2022) and RBM (Blaskey, 2024a) were used to produce the full simulation results (Blaskey, 2023) after the model underwent optimization (Blaskey, 2024b). Discharge and temperature data for the US State of Alaska were collected from the United States Geological Survey National Water Information System (U.S. Geological Survey, 2022) and are permanently stored in the software published by Blaskey (2024b). These were the historical observational data sets used for model evaluation in this research. ERA5 data were used to calibrate the climate model (Muñoz Sabater, 2019).

Acknowledgments
We would like to thank Dr. Balaji Rajagopalan for providing the idea of using a statistical benchmark model and Dr. Ben Livneh who provided us guidance on the model calibration. This material is based upon work supported by the National Science Foundation Navigating the New Arctic Grant 1928189 for the University of Colorado and 1928078 for the National Center for Atmospheric Research, which is sponsored by the National Science Foundation under Cooperative Agreement No. 1852977. JCK was funded by the Changing Arctic Ecosystems Initiative of the Wildlife program of the U.S. Geological Survey Ecosystems Mission Area. Any use of trade, film, or product names is for descriptive purposes only and do not imply endorsement by the U.S. Government. We would like to acknowledge high-performance computing support from Cheyenne (https://doi.org/10.5065/D6RX99HX) provided by NCAR's Computational and Information Systems Laboratory, sponsored by the National Science Foundation.

References

Abramowitz, G. (2005). Towards a benchmark for land surface models. *Geophysical Research Letters*, *32*(22), L22702. https://doi.org/10.1029/2005gl024419

Benyahya, L., Caissie, D., El-Jabi, N., & Satish, M. G. (2010). Comparison of microclimate vs. remote meteorological data and results applied to a water temperature model (Miramichi River, Canada). *Journal of Hydrology*, *380*(3–4), 247–259. https://doi.org/10.1016/j.jhydrol.2009.10.039

Best, M. J., Abramowitz, G., Johnson, H. R., Pitman, A. J., Balsamo, G., Boone, A., et al. (2015). The plumbing of land surface models: Benchmarking model performance. *Journal of Hydrometeorology*, *16*(3), 1425–1442. https://doi.org/10.1175/jhm-d-14-0158.1

Bieniek, P. A., Walsh, J. E., Thoman, R. L., & Bhatt, U. S. (2014). Using climate divisions to analyze variations and trends in Alaska temperature and precipitation. *Journal of Climate*, *27*(8), 2800–2818. https://doi.org/10.1175/jcli-d-13-00342.1

Blaskey, D. (2023). High-resolution, daily hindcast (1990–2021) data of Alaskan river discharge and temperature [Dataset]. *Zenodo*. https://doi.org/10.5281/zenodo.8320319

Blaskey, D. (2024a). RASM-mizuRoute-RBM-1.0: January 30, 2024. Release (Version 1.0) [Software]. *Zenodo*. Retrieved from https://zenodo.org/doi/10.5281/zenodo.10593447

Blaskey, D. (2024b). dblaskey/RBM_Optimization: RBM optimization framework: January 30, 2024. Release (Version 1.0) [Software]. *Zenodo*. Retrieved from https://zenodo.org/doi/10.5281/zenodo.10593427

Blaskey, D., Koch, J. C., Gooseff, M. N., Newman, A. J., Cheng, Y., O'Donnell, J. A., & Musselman, K. N. (2023). Increasing Alaskan river discharge during the cold season is driven by recent warming. *Environmental Research Letters*, *18*(2), 024042. https://doi.org/10.1088/1748-9326/acb661

Bolduc, C., & Lamoureux, S. F. (2018). Multiyear variations in High Arctic river temperatures in response to climate variability. *Arctic Science*, *4*(4), 605–623. https://doi.org/10.1139/as-2017-0053

Bonyadi, M. R., & Michalewicz, Z. (2017). Particle swarm optimization for single objective continuous space problems: A review. *Evolutionary Computation*, *25*(1), 1–54. https://doi.org/10.1162/evco_r_00180

Boussaïd, I., Lepagnot, J., & Siarry, P. (2013). A survey on optimization metaheuristics. *Information Sciences*, *237*, 82–117. https://doi.org/10.1016/j.ins.2013.02.041

Brown, L. E., & Hannah, D. M. (2008). Spatial heterogeneity of water temperature across an alpine river basin. *Hydrological Processes: An International Journal*, *22*(7), 954–967. https://doi.org/10.1002/hyp.6982

Burkholder, B. K., Grant, G. E., Haggerty, R., Khangaonkar, T., & Wampler, P. J. (2008). Influence of hyporheic flow and geomorphology on temperature of a large, gravel-bed river, Clackamas River, Oregon, USA. *Hydrological Processes: An International Journal*, *22*(7), 941–953. https://doi.org/10.1002/hyp.6984

Caissie, D. (2006). The thermal regime of rivers: A review. *Freshwater Biology*, *51*(8), 1389–1406. https://doi.org/10.1111/j.1365-2427.2006.01597.x

Carothers, C., Black, J., Langdon, S. J., Donkersloot, R., Ringer, D., Coleman, J., et al. (2021). Indigenous peoples and salmon stewardship: A critical relationship. *Ecology and Society*, *26*(1), 16. https://doi.org/10.5751/ES-11972-260116

Cheng, Y., Musselman, K. N., Swenson, S., Lawrence, D., Hamman, J., Dagon, K., et al. (2023). Moving land models toward more actionable science: A novel application of the community terrestrial systems model across Alaska and the Yukon River basin. *Water Resources Research*, *59*(1), e2022WR032204. https://doi.org/10.1029/2022wr032204

Cheng, Y., Voisin, N., Yearsley, J. R., & Nijssen, B. (2020). Reservoirs modify river thermal regime sensitivity to climate change: A case study in the southeastern United States. *Water Resources Research*, *56*(6), e2019WR025784. https://doi.org/10.1029/2019wr025784

Chikita, K. A., Kaminaga, R., Kudo, I., Wada, T., & Kim, Y. (2010). Parameters determining water temperature of a proglacial stream: The Phelan Creek and the Gulkana Glacier, Alaska. *River Research and Applications*, *26*(8), 995–1004. https://doi.org/10.1002/rra.1311

Clausius, R. (1850). Ueber die bewegende Kraft der Wärme und die Gesetze, welche sich daraus für die Wärmelehre selbst ableiten lassen. *Annalen der Physik*, *155*(3), 368–397. https://doi.org/10.1002/andp.18501550403

Computational and Information Systems Laboratory. (2019). *Cheyenne: HPE/SGI ICE XA System (NCAR Community Computing)*. National Center for Atmospheric Research. https://doi.org/10.5065/D6RX99HX

Coutant, C. C. (1999). *Perspectives on temperature in the Pacific Northwest's fresh waters* (No. ORNL/TM-1999/44). Oak Ridge National Lab. (ORNL).

Cozzetto, K. D., Bencala, K. E., Gooseff, M. N., & McKnight, D. M. (2013). The influence of stream thermal regimes and preferential flow paths on hyporheic exchange in a glacial meltwater stream. *Water Resources Research*, *49*(9), 5552–5569. https://doi.org/10.1002/wrcr.20410

Cozzetto, K. D., McKnight, D., Nylen, T., & Fountain, A. (2006). Experimental investigations into processes controlling stream and hyporheic temperatures, Fryxell Basin, Antarctica. *Advances in Water Resources*, *29*(2), 130–153. https://doi.org/10.1016/j.advwatres.2005.04.012

Crossman, J., Futter, M. N., & Whitehead, P. G. (2013). The significance of shifts in precipitation patterns: Modelling the impacts of climate change and glacier retreat on extreme flood events in Denali National Park, Alaska. *PLoS One*, *8*(9), e74054. https://doi.org/10.1371/journal.pone.0074054

Curran, J. H., & Biles, F. E. (2021). Identification of seasonal streamflow regimes and streamflow drivers for daily and peak flows in Alaska. *Water Resources Research*, *57*(2), e2020WR028425. https://doi.org/10.1029/2020wr028425

Das, P. K., Behera, H. S., & Panigrahi, B. K. (2016). A hybridization of an improved particle swarm optimization and gravitational search algorithm for multi-robot path planning. *Swarm and Evolutionary Computation*, *28*, 14–28. https://doi.org/10.1016/j.swevo.2015.10.011

Deb, K., Pratap, A., Agarwal, S., & Meyarivan, T. A. M. T. (2002). A fast and elitist multiobjective genetic algorithm: NSGA-II. *IEEE Transactions on Evolutionary Computation*, *6*(2), 182–197. https://doi.org/10.1109/4235.996017

DeCicco, L., Hirsch, R., Lorenz, D., Watkins, D., & Johnson, M. (2023). dataRetrieval: R packages for discovering and retrieving water data available from U.S. federal hydrologic web services. https://doi.org/10.5066/P9X4L3GE

Dugdale, S. J., Bergeron, N. E., & St-Hilaire, A. (2015). Spatial distribution of thermal refuges analysed in relation to riverscape hydromorphology using airborne thermal infrared imagery. *Remote Sensing of Environment*, *160*, 43–55. https://doi.org/10.1016/j.rse.2014.12.021

Dugdale, S. J., Hannah, D. M., & Malcolm, I. A. (2017). River temperature modelling: A review of process-based approaches and future directions. *Earth-Science Reviews*, *175*, 97–113. https://doi.org/10.1016/j.earscirev.2017.10.009

Durance, I., & Ormerod, S. J. (2009). Trends in water quality and discharge confound long-term warming effects on river macroinvertebrates. *Freshwater Biology*, *54*(2), 388–405. https://doi.org/10.1111/j.1365-2427.2008.02112.x

Fabris, L., Rolick, R. L., Kurylyk, B. L., & Carey, S. K. (2020). Characterization of contrasting flow and thermal regimes in two adjacent subarctic alpine headwaters in Northwest Canada. *Hydrological Processes*, *34*(15), 3252–3270. https://doi.org/10.1002/hyp.13786

Fan, Y., Clark, M., Lawrence, D. M., Swenson, S., Band, L. E., Brantley, S. L., et al. (2019). Hillslope hydrology in global change research and Earth System Modeling. *Water Resources Research*, *55*(2), 1737–1772. https://doi.org/10.1029/2018WR023903

Ferchichi, H., & St-Hilaire, A. (2023). Are temperature time series measured at hydrometric stations representative of the river's thermal regime? *Canadian Water Resources Journal/Revue Canadienne des Ressources Hydriques*, *48*(2), 1–18. https://doi.org/10.1080/07011784.2023.2216454

Ficklin, D. L., Luo, Y., Stewart, I. T., & Maurer, E. P. (2012). Development and application of a hydroclimatological stream temperature model within the Soil and Water Assessment Tool. *Water Resources Research*, *48*(1), 1–16. https://doi.org/10.1029/2011wr011256

Frechette, D. M., Dugdale, S. J., Dodson, J. J., & Bergeron, N. E. (2018). Understanding summertime thermal refuge use by adult Atlantic salmon using remote sensing, river temperature monitoring, and acoustic telemetry. *Canadian Journal of Fisheries and Aquatic Sciences*, *75*(11), 1999–2010. https://doi.org/10.1139/cjfas-2017-0422

Giorgi, F. (2019). Thirty years of regional climate modeling: Where are we and where are we going next? *Journal of Geophysical Research: Atmospheres*, *124*(11), 5696–5723. https://doi.org/10.1029/2018jd030094

Gong, D., Sun, J., & Miao, Z. (2016). A set-based genetic algorithm for interval many-objective optimization problems. *IEEE Transactions on Evolutionary Computation*, *22*(1), 47–60. https://doi.org/10.1109/tevc.2016.2634625

Gu, R., Montgomery, S., & Austin, T. A. (1998). Quantifying the effects of stream discharge on summer river temperature. *Hydrological Sciences Journal*, *43*(6), 885–904. https://doi.org/10.1080/02626669809492185

Guenther, S. M., Moore, R. D., & Gomi, T. (2012). Riparian microclimate and evaporation from a coastal headwater stream, and their response to partial-retention forest harvesting. *Agricultural and Forest Meteorology*, *164*, 1–9. https://doi.org/10.1016/j.agrformet.2012.05.003

Gupta, H. V., Kling, H., Yilmaz, K. K., & Martinez, G. F. (2009). Decomposition of the mean squared error and NSE performance criteria: Implications for improving hydrological modelling. *Journal of Hydrology*, *377*(1–2), 80–91. https://doi.org/10.1016/j.jhydrol.2009.08.003

Isaak, D. J., Wenger, S. J., Peterson, E. E., Ver Hoef, J. M., Nagel, D. E., Luce, C. H., et al. (2017). The NorWeST summer stream temperature model and scenarios for the western US: A crowd-sourced database and new geospatial tools foster a user community and predict broad climate warming of rivers and streams. *Water Resources Research*, *53*(11), 9181–9205. https://doi.org/10.1002/2017wr020969

Kaushal, S. S., Likens, G. E., Jaworski, N. A., Pace, M. L., Sides, A. M., Seekell, D., et al. (2010). Rising stream and river temperatures in the United States. *Frontiers in Ecology and the Environment*, *8*(9), 461–466. https://doi.org/10.1890/090037

King, T. V., & Neilson, B. T. (2019). Quantifying reach-average effects of hyporheic exchange on Arctic river temperatures in an area of continuous permafrost. *Water Resources Research*, *55*(3), 1951–1971. https://doi.org/10.1029/2018wr023463

Koch, J. C., Sjöberg, Y., O'Donnell, J. A., Carey, M. P., Sullivan, P. F., & Terskaia, A. (2022). Sensitivity of headwater streamflow to thawing permafrost and vegetation change in a warming Arctic. *Environmental Research Letters*, *17*(4), 044074. https://doi.org/10.1088/1748-9326/ac5f2d

Lawrence, D. M., Fisher, R. A., Koven, C. D., Oleson, K. W., Swenson, S. C., Bonan, G., et al. (2019). The Community Land Model version 5: Description of new features, benchmarking, and impact of forcing uncertainty. *Journal of Advances in Modeling Earth Systems*, *11*(12), 4245–4287. https://doi.org/10.1029/2018ms001583

Leach, J. A., Kelleher, C., Kurylyk, B. L., Moore, R. D., & Neilson, B. T. (2023). A primer on stream temperature processes. *Wiley Interdisciplinary Reviews: Water*, *10*(4), e1643. https://doi.org/10.1002/wat2.1643

Leach, J. A., & Moore, R. D. (2010). Above-stream microclimate and stream surface energy exchanges in a wildfire-disturbed riparian zone. *Hydrological Processes*, *24*(17), 2369–2381. https://doi.org/10.1002/hyp.7639

Leach, J. A., & Moore, R. D. (2019). Empirical stream thermal sensitivities may underestimate stream temperature response to climate warming. *Water Resources Research*, *55*(7), 5453–5467. https://doi.org/10.1029/2018wr024236

Lee, S. Y., Fullerton, A. H., Sun, N., & Torgersen, C. E. (2020). Projecting spatiotemporally explicit effects of climate change on stream temperature: A model comparison and implications for coldwater fishes. *Journal of Hydrology*, *588*, 125066. https://doi.org/10.1016/j.jhydrol.2020.125066

Lehner, F., Wood, A. W., Vano, J. A., Lawrence, D. M., Clark, M. P., & Mankin, J. S. (2019). The potential to reduce uncertainty in regional runoff projections from climate models. *Nature Climate Change*, *9*(12), 926–933. https://doi.org/10.1038/s41558-019-0639-x

Leopold, L. B., & Maddock, T. (1953). *The hydraulic geometry of stream channels and some physiographic implications* (Vol. 252). US Government Printing Office.
Li, C., Wei, Y., Liu, Y., Li, L., Peng, L., Chen, J., et al. (2022). Active layer thickness in the Northern Hemisphere: Changes from 2000 to 2018 and future simulations. *Journal of Geophysical Research: Atmospheres*, *127*(12), e2022JD036785. https://doi.org/10.1029/2022jd036785
Manning, R., Griffith, J. P., Pigot, T. F., & Vernon-Harcourt, L. F. (1890). On the flow of water in open channels and pipes.
Mantua, N., Tohver, I., & Hamlet, A. (2010). Climate change impacts on streamflow extremes and summertime stream temperature and their possible consequences for freshwater salmon habitat in Washington State. *Climatic Change*, *102*(1–2), 187–223. https://doi.org/10.1007/s10584-010-9845-2
Mayer, N. B., Hinch, S. G., & Eliason, E. J. (2023). Thermal tolerance in Pacific salmon: A systematic review of species, populations, life stages and methodologies. *Fish and Fisheries*, *25*(2), 283–302. https://doi.org/10.1111/faf.12808
McKay, M. D., Beckman, R. J., & Conover, W. J. (2000). A comparison of three methods for selecting values of input variables in the analysis of output from a computer code. *Technometrics*, *42*(1), 55–61. https://doi.org/10.2307/1271432
Mizukami, N., Clark, M. P., Newman, A. J., Wood, A. W., Gutmann, E. D., Nijssen, B., et al. (2017). Towards seamless large-domain parameter estimation for hydrologic models. *Water Resources Research*, *53*(9), 8020–8040. https://doi.org/10.1002/2017WR020401
Mizukami, N., Clark, M. P., Nijssen, B., & Gharari, S. (2022). ESCOMP/mizuRoute: v1.2.1: July 17, 2022. Release (Version v1.2.2) [Software]. *Zenodo*. https://doi.org/10.5281/zenodo.6851192
Mizukami, N., Clark, M. P., Sampson, K., Nijssen, B., Mao, Y., McMillan, H., et al. (2016). mizuRoute version 1: A river network routing tool for a continental domain water resources applications. *Geoscientific Model Development*, *9*(6), 2223–2238. https://doi.org/10.5194/gmd-9-2223-2016
Mohseni, O., Stefan, H. G., & Erickson, T. R. (1998). A nonlinear regression model for weekly stream temperatures. *Water Resources Research*, *34*(10), 2685–2692. https://doi.org/10.1029/98wr01877
Monaghan, A. J., Clark, M. P., Barlage, M. P., Newman, A. J., Xue, L., Arnold, J. R., & Rasmussen, R. M. (2018). High-resolution historical climate simulations over Alaska. *Journal of Applied Meteorology and Climatology*, *57*(3), 709–731. https://doi.org/10.1175/jamc-d-17-0161.1
Muñoz Sabater, J. (2019). ERA5-Land hourly data from 1950 to present [Dataset]. *Copernicus Climate Change Service (C3S)*. https://doi.org/10.24381/cds.e2161bac
Musselman, K. N., Addor, N., Vano, J. A., & Molotch, N. P. (2021). Winter melt trends portend widespread declines in snow water resources. *Nature Climate Change*, *11*(5), 418–424. https://doi.org/10.1038/s41558-021-01014-9
Newman, A. J., Mizukami, N., Clark, M. P., Wood, A. W., Nijssen, B., & Nearing, G. (2017). Benchmarking of a physically based hydrologic model. *Journal of Hydrometeorology*, *18*(8), 2215–2225. https://doi.org/10.1175/jhm-d-16-0284.1
Nielsen, J. L., Lisle, T. E., & Ozaki, V. (1994). Thermally stratified pools and their use by steelhead in northern California streams. *Transactions of the American Fisheries Society*, *123*(4), 613–626. https://doi.org/10.1577/1548-8659(1994)123<0613:tspatu>2.3.co;2
Niemeyer, R. J., Cheng, Y., Mao, Y., Yearsley, J. R., & Nijssen, B. (2018). A thermally stratified reservoir module for large-scale distributed stream temperature models with application in the Tennessee River basin. *Water Resources Research*, *54*(10), 8103–8119. https://doi.org/10.1029/2018wr022615
Oke, K. B., Cunningham, C. J., Westley, P. A. H., Baskett, M. L., Carlson, S. M., Clark, J., et al. (2020). Recent declines in salmon body size impact ecosystems and fisheries. *Nature Communications*, *11*(1), 4155. https://doi.org/10.1038/s41467-020-17726-z
Piotrowski, A. P., & Napiorkowski, J. J. (2018). Performance of the air2stream model that relates air and stream water temperatures depends on the calibration method. *Journal of Hydrology*, *561*, 395–412. https://doi.org/10.1016/j.jhydrol.2018.04.016
Pörtner, H. O., & Farrell, A. P. (2008). Physiology and climate change. *Science*, *322*(5902), 690–692. https://doi.org/10.1126/science.1163156
Rantanen, M., Karpechko, A. Y., Lipponen, A., Nordling, K., Hyvärinen, O., Ruosteenoja, K., et al. (2022). The Arctic has warmed nearly four times faster than the globe since 1979. *Communications Earth & Environment*, *3*(1), 168. https://doi.org/10.1038/s43247-022-00498-3
R Core Team. (2022). *R: A language and environment for statistical computing*. R Foundation for Statistical Computing. Retrieved from https://www.R-project.org/
Reder, A., Raffa, M., Montesarchio, M., & Mercogliano, P. (2020). Performance evaluation of regional climate model simulations at different spatial and temporal scales over the complex orography area of the Alpine region. *Natural Hazards*, *102*(1), 151–177. https://doi.org/10.1007/s11069-020-03916-x
Ruesch, A. S., Torgersen, C. E., Lawler, J. J., Olden, J. D., Peterson, E. E., Volk, C. J., & Lawrence, D. J. (2012). Projected climate-induced habitat loss for salmonids in the John Day River network, Oregon, USA. *Conservation Biology*, *26*(5), 873–882. https://doi.org/10.1111/j.1523-1739.2012.01897.x
Sjöberg, Y., Jan, A., Painter, S. L., Coon, E. T., Carey, M. P., O'Donnell, J. A., & Koch, J. C. (2021). Permafrost promotes shallow groundwater flow and warmer headwater streams. *Water Resources Research*, *57*(2), e2020WR027463. https://doi.org/10.1029/2020wr027463
Skamarock, W. C., Klemp, J. B., Dudhia, J., Gill, D. O., Liu, Z., Berner, J., et al., (2019). A description of the advanced research WRF Version 4. NCAR Tech. Note NCAR/TN-556+STR (pp. 145). https://doi.org/10.5065/1dfh-6p97
Steel, E. A., Beechie, T. J., Torgersen, C. E., & Fullerton, A. H. (2017). Envisioning, quantifying, and managing thermal regimes on river networks. *BioScience*, *67*(6), 506–522. https://doi.org/10.1093/biosci/bix047
Sun, N., Yearsley, J., Voisin, N., & Lettenmaier, D. P. (2015). A spatially distributed model for the assessment of land use impacts on stream temperature in small urban watersheds. *Hydrological Processes*, *29*(10), 2331–2345. https://doi.org/10.1002/hyp.10363
Swenson, S. C., Clark, M., Fan, Y., Lawrence, D. M., & Perket, J. (2019). Representing intrahillslope lateral subsurface flow in the Community Land Model. *Journal of Advances in Modeling Earth Systems*, *11*(12), 4044–4065. https://doi.org/10.1029/2019MS001833
Tayfur, G. (2017). Modern optimization methods in water resources planning, engineering and management. *Water Resources Management*, *31*(10), 3205–3233. https://doi.org/10.1007/s11269-017-1694-6
Tisseuil, C., Vrac, M., Grenouillet, G., Wade, A. J., Gevrey, M., Oberdorff, T., et al. (2012). Strengthening the link between climate, hydrological and species distribution modeling to assess the impacts of climate change on freshwater biodiversity. *Science of the Total Environment*, *424*, 193–201. https://doi.org/10.1016/j.scitotenv.2012.02.035
Tornabene, B. J., Smith, T. W., Tews, A. E., Beattie, R. P., Gardner, W. M., & Eby, L. A. (2020). Trends in river discharge and water temperature cue spawning movements of blue sucker, Cycleptus elongatus, in an impounded Great Plains River. *Copeia*, *108*(1), 151–162. https://doi.org/10.1643/ci-19-256
Tung, C. P., Lee, T. Y., & Yang, Y. C. (2006). Modelling climate-change impacts on stream temperature of Formosan landlocked salmon habitat. *Hydrological Processes: An International Journal*, *20*(7), 1629–1649. https://doi.org/10.1002/hyp.5959
U.S. Geological Survey. (2022). *USGS water data for the Nation*. U.S. Geological Survey National Water Information System database. https://doi.org/10.5066/F7P55KJN

van Vliet, M. T. H., Franssen, W. H., Yearsley, J. R., Ludwig, F., Haddeland, I., Lettenmaier, D. P., & Kabat, P. (2013). Global river discharge and water temperature under climate change. *Global Environmental Change*, *23*(2), 450–464. https://doi.org/10.1016/j.gloenvcha.2012.11.002

van Vliet, M. T. H., Ludwig, F., Zwolsman, J. J. G., Weedon, G. P., & Kabat, P. (2011). Global river temperatures and sensitivity to atmospheric warming and changes in river flow. *Water Resources Research*, *47*(2), W02544. https://doi.org/10.1029/2010wr009198

van Vliet, M. T. H., Yearsley, J. R., Franssen, W. H. P., Ludwig, F., Haddeland, I., Lettenmaier, D. P., & Kabat, P. (2012). Coupled daily streamflow and water temperature modelling in large river basins. *Hydrology and Earth System Sciences*, *16*(11), 4303–4321. https://doi.org/10.5194/hess-16-4303-2012

von Biela, V. R., Sergeant, C. J., Carey, M. P., Liller, Z., Russell, C., Quinn-Davidson, S., et al. (2022). Premature mortality observations among Alaska's Pacific Salmon during record heat and drought in 2019. *Fisheries*, *47*(4), 157–168. https://doi.org/10.1002/fsh.10705

Wagner, R. J., Boulger Jr, R. W., Oblinger, C. J., & Smith, B. A. (2006). Guidelines and standard procedures for continuous water-quality monitors: Station operation, record computation, and data reporting (No. 1-D3).

Wanders, N., van Vliet, M. T., Wada, Y., Bierkens, M. F., & van Beek, L. P. (2019). High-resolution global water temperature modeling. *Water Resources Research*, *55*(4), 2760–2778. https://doi.org/10.1029/2018wr023250

Wang, G. G., Hossein Gandomi, A., Yang, X. S., & Hossein Alavi, A. (2014). A novel improved accelerated particle swarm optimization algorithm for global numerical optimization. *Engineering Computations*, *31*(7), 1198–1220. https://doi.org/10.1108/ec-10-2012-0232

Watts, G., Battarbee, R. W., Bloomfield, J. P., Crossman, J., Daccache, A., Durance, I., et al. (2015). Climate change and water in the UK–past changes and future prospects. *Progress in Physical Geography*, *39*(1), 6–28. https://doi.org/10.1177/0309133314542957

Wondzell, S. M., Diabat, M., & Haggerty, R. (2019). What matters most: Are future stream temperatures more sensitive to changing air temperatures, discharge, or riparian vegetation? *JAWRA Journal of the American Water Resources Association*, *55*(1), 116–132. https://doi.org/10.1111/1752-1688.12707

Yamazaki, D., Ikeshima, D., Sosa, J., Bates, P. D., Allen, G. H., & Pavelsky, T. M. (2019). MERIT Hydro: A high-resolution global hydrography map based on latest topography dataset. *Water Resources Research*, *55*(6), 5053–5073. https://doi.org/10.1029/2019wr024873

Yan, H., Sun, N., Fullerton, A., & Baerwalde, M. (2021). Greater vulnerability of snowmelt-fed river thermal regimes to a warming climate. *Environmental Research Letters*, *16*(5), 054006. https://doi.org/10.1088/1748-9326/abf393

Yang, R., Hock, R., Kang, S., Shangguan, D., & Guo, W. (2020). Glacier mass and area changes on the Kenai Peninsula, Alaska, 1986–2016. *Journal of Glaciology*, *66*(258), 603–617. https://doi.org/10.1017/jog.2020.32

Yearsley, J. R. (2009). A semi-Lagrangian water temperature model for advection-dominated river systems. *Water Resources Research*, *45*(12), W12405. https://doi.org/10.1029/2008wr007629

Yearsley, J. R. (2012). A grid-based approach for simulating stream temperature. *Water Resources Research*, *48*(3), 1. https://doi.org/10.1029/2011wr011515

Zheng, L., Overeem, I., Wang, K., & Clow, G. D. (2019). Changing Arctic river dynamics cause localized permafrost thaw. *Journal of Geophysical Research: Earth Surface*, *124*(9), 2324–2344. https://doi.org/10.1029/2019jf005060

References From the Supporting Information

Jorgenson, M. T., Yoshikawa, K., Kanevskiy, M., Shur, Y., Romanovsky, V., Marchenko, S., et al. (2008). Permafrost characteristics of Alaska. In *Proceedings of the ninth international conference on permafrost* (Vol. 3, pp. 121–122). University of Alaska.